# Response of an aerosol mass spectrometer to organonitrates and organosulfates and implications for atmospheric chemistry

D. K. Farmer[a], A. Matsunaga[b], K. S. Docherty[a], J. D. Surratt[c], J. H. Seinfeld[c,d], P. J. Ziemann[b], and J. L. Jimenez[a,1]

[a]Cooperative Institute for Research in Environmental Sciences and Department of Chemistry and Biochemistry, University of Colorado, Boulder, CO 80309; [b]Air Pollution Research Center and Department of Chemistry, University of California, Riverside, CA 92521; [c]Division of Chemistry and Chemical Engineering, California Institute of Technology, Pasadena, CA 91125; and [d]Division of Engineering and Applied Science, California Institute of Technology, Pasadena, CA 91125

Edited by Barbara J. Finlayson-Pitts, University of California, Irvine, CA, and approved January 29, 2010 (received for review October 25, 2009)

**Organonitrates (ON) are important products of gas-phase oxidation of volatile organic compounds in the troposphere; some models predict, and laboratory studies show, the formation of large, multifunctional ON with vapor pressures low enough to partition to the particle phase. Organosulfates (OS) have also been recently detected in secondary organic aerosol. Despite their potential importance, ON and OS remain a nearly unexplored aspect of atmospheric chemistry because few studies have quantified particulate ON or OS in ambient air. We report the response of a high-resolution time-of-flight aerosol mass spectrometer (AMS) to aerosol ON and OS standards and mixtures. We quantify the potentially substantial underestimation of organic aerosol O/C, commonly used as a metric for aging, and N/C. Most of the ON-nitrogen appears as $NO_x^+$ ions in the AMS, which are typically dominated by inorganic nitrate. Minor organonitrogen ions are observed although their identity and intensity vary between standards. We evaluate the potential for using $NO_x^+$ fragment ratios, organonitrogen ions, $HNO_3^+$ ions, the ammonium balance of the nominally inorganic ions, and comparison to ion-chromatography instruments to constrain the concentrations of ON for ambient datasets, and apply these techniques to a field study in Riverside, CA. OS manifests as separate organic and sulfate components in the AMS with minimal organosulfur fragments and little difference in fragmentation from inorganic sulfate. The low thermal stability of ON and OS likely causes similar detection difficulties for other aerosol mass spectrometers using vaporization and/or ionization techniques with similar or larger energy, which has likely led to an underappreciation of these species.**

atmospheric chemistry | organic aerosol | organic nitrate | organic sulfate | SOA

Organonitrates (ON, i.e., $RONO_2$) and organosulfates (OS, i.e., $ROSO_3H$) are known to be present in secondary organic aerosol (SOA) (1–4), and are a nearly unexplored but potentially important aspect of atmospheric chemistry. The mechanisms behind ON and OS production and aging are poorly understood and generally ignored in models due in part to a lack of measurement approaches. ON have recently been identified as significant components (15–35%) of $NO_y$ in the gas-phase (5, 6) and serve as indicators of ozone production (7). Oceans and certain industrial processes directly emit ON, but these are generally short-chain alkyl nitrates that exist only in the gas-phase and constitute a minor fraction of atmospheric ON (6, 8). Most atmospheric ON are produced either by photochemical (OH-initiated) or nocturnal ($NO_3$-initiated) oxidation reactions of anthropogenic and biogenic volatile organic compounds (VOCs). These reactions can produce large, multifunctional ON with vapor pressures potentially low enough to condense and form SOA. During photochemical oxidation of VOCs in the presence of nitrogen oxides, ON are minor products of peroxy radical $(RO_2) + NO$ reactions. These reactions produce ON with yields of 0–30%, depending on the size and structure of the VOC precursor (9). Larger VOCs typically have greater ON yields and result in ON with lower vapor pressures. ON from $NO_3$ oxidation of isoprene and monoterpenes have been suggested to be a substantial biogenic SOA source (1, 2). Despite several laboratory and modeling studies demonstrating particulate ON production (1, 2, 10–13), these species have not been conclusively demonstrated to be a significant component of ambient SOA, and are thus often not considered in SOA models. Model studies including ON production have suggested that photochemical ON production accounts for a substantial fraction of SOA functionalization, with estimates that 18% of SOA molecules possess nitrate groups (10).

The lack of observational constraints on particulate ON is due to limitations of the existing analysis methods. Off-line analysis of impactors by FTIR provides a time-averaged indication of ON (14), but interferences are possible (15), and ON are often below FTIR detection limit even in highly polluted environments (16). On the basis of 24-hr averaged filter samples analyzed by FTIR, particulate ON accounted for approximately 0.25% of total $NO_y$ at a Danish agricultural site, compared to the 7% of gas-phase ON (17). Real-time instruments tend to sacrifice chemical specificity for time resolution. Thermal dissociation–laser induced fluorescence (TD-LIF) measures the sum of gaseous and particulate ON and can thus produce an upper bound on particulate ON (18). Total particulate organic N has also been recently estimated as the difference between total N and inorganic N, defined as soluble nitrate-N plus ammonium-N (19). This method cannot distinguish between reduced and oxidized organic N, but can provide an upper limit of ambient particulate ON. For example, at the Duke Forest site in North Carolina, 33% of the total N in $PM_{2.5}$ was estimated to be organic, though this was not classified into ON versus amines or other organic N. The relative partitioning of ON into particle vs. gas-phase and the contribution of ON to SOA remain open, but important, questions. Alternately, if ON are not present in aerosols to the extent predicted, then other atmospheric loss processes need to be considered, including reaction with OH to release $NO_2$, rapid gas-phase deposition, photolysis, or reactive conversion to other species, such as $HNO_3$ and organics.

OS (i.e., $ROSO_3H$) have been observed in both laboratory-generated and ambient organic aerosol (OA) using negative ion (−) electrospray ionization (ESI)-MS techniques, resulting

Author contributions: D.K.F. and J.L.J. designed research; D.K.F. and A.M. performed research; A.M., J.D.S., J.H.S., and P.J.Z. contributed new reagents/analytic tools; D.K.F., K.S.D., and J.L.J. analyzed data; and D.K.F. and J.L.J. wrote the paper.

The authors declare no conflict of interest.

This article is a PNAS Direct Submission.

[1]To whom correspondence should be addressed at: University of Colorado, UCB 216, Boulder, CO 80309. E-mail: jose.jimenez@colorado.edu.

This article contains supporting information online at www.pnas.org/cgi/content/full/0912340107/DCSupplemental.

in the understanding that OS form in ambient aerosol from the oxidation of biogenic VOC in the presence of acidified sulfate aerosol (4, 20). Although their prevalence in ambient aerosol remains unclear, further evidence for substantial OS contributions to SOA come from rainwater studies (21). Similar to ON, OS have been quantified as the difference between total particulate S and sulfate plus methylsulfonic acid (MSA); studies in rural Hungary estimated OS accounted for 6–14% of sulfate (22) and up to 30% of the total organic matter (23). OS fractions of this order would cause an error in the evaluation of acidity using nominally inorganic ions (24) and constitute a fraction of OA that is not accounted for in current models. Further, while chamber studies have focused on OS formation from the uptake of biogenic VOC oxidation products on acidified sulfate aerosol (4, 20, 23), anthropogenic VOC oxidation products likely also form OS.

Aerosol mass spectrometers (AMS) have been used to quantify OA and its sources in numerous field campaigns (25, 26) and have the advantage over other bulk particle measurement techniques of fast time resolution coupled with quantitative, real-time chemical speciation and size resolution. Recently, the ability to quantify the elemental composition of OA with the high-mass-resolution version of the AMS (HR-AMS) has been demonstrated (27, 28). However, its response to particulate ON and OS has not been fully characterized; the AMS uses electron ionization (EI), which leads to substantial fragmentation of OA molecules. Chamber experiments suggest that ON produce $NO^+$ and $NO_2^+$ fragments in the AMS (1, 13), which would cause underestimates of O/C and N/C in ambient studies in which such ions are typically not assumed to arise from OA. Similarly, OS are expected to produce $H_xSO_y^+$ ions (20), which would cause underestimates in O/C and S/C ratios in ambient studies. Previous application of the AMS to particulate ON and OS measurements have been limited to laboratory studies in which no other N- or S-containing species were expected to be present in the aerosol phase (1, 13, 20).

Here, we present a detailed analysis of the response of an HR-AMS to particulate ON and OS standards and bracket their contribution to ambient OA in Riverside, CA during the Study of Organic Aerosols in Riverside (SOAR-1) campaign. A difficulty in identifying these species is revealed, which is also relevant to many other instruments used in ambient studies that use similar or more energetic vaporization and/or ionization techniques as part of the analysis. This finding may help explain the relative lack of information on ON and OS in ambient aerosols.

## Results

**Organonitrates.** Table S1 and Figs. S1–S6 summarize fragmentation of ON standards in the HR-AMS; particulate ON were detected in both the HR-AMS organic and nitrate signals, due to decomposition in either or both the vaporization or ionization stage of the AMS. ON standards were dominantly observed as separate "organic" ($C_xH_yO_z^+$, $C_xH_y^+$) and "nitrate" ($H_xN_yO_z^+$) fragments, with few (approximately 5% of the ON-nitrogen signal at 600 °C) organonitrogen ($C_xH_yO_zN_p^+$) fragments (Fig. 1*A*). The identity of the dominant organonitrogen fragments depends on the standard, consistent with other studies (13) and our understanding of fragmentation following EI. Reduced nitrogen ($NH_y$) ions accounted for an average of $1.8 \pm 0.4\%$ of the N signal in the ON standards (vaporizer temperature, $T_v = 600$ °C), likely from impurities in the analysis. Neither $C_xH_yN_p^+$ ions (organonitrogen ions without O) nor organonitrogen ions with more than one N were observed. The relative contribution of organonitrogen fragments to total detected N increased in the dihydroxynitrate standard as $T_v$ was lowered, although the extent to which this occurs for other standards is unclear. Organonitrogen ions represent <1% of the total observed organic signal even though C-$ONO_2$ comprise 6–8% of the carbon atoms. The response of the HR-AMS to the ON standards reported here has important implications for interpretation of ambient AMS data: first, the carbon skeleton of the ON is included in OA concentration. Second, if ON are present, the nitrate reported by the standard AMS software cannot be considered entirely inorganic; this will affect estimates of not only aerosol acidity, but also of OA oxidation state.

Elemental analysis of the ON standards, including both the organic and nitrate components, underestimates O/C, H/C, and N/C ratios relative to predicted, although mostly within the uncertainty (28) typically observed for organic standards (Table S1). However, because ON fragment into nitrate components typically considered inorganic, the presence of ON in ambient aerosol has implications to HR-AMS elemental analysis of OA. Typical HR-AMS ambient OA elemental analysis includes only the organic fraction, and thus O/C and N/C ratios will be underestimated in the presence of ON, as quantified below.

**Organosulfates.** Only one OS standard (trihydroxy sulfate ester of isoprene) was successfully analyzed with the HR-AMS, possibly as other standards tested (e.g., hydroxy sulfate esters of α- and β-pinene) were either present in very low concentrations or were lost in the nebulizer or transfer lines before the HR-AMS. Similar to ON, the OS standard fragmented almost completely to "nominally sulfate" ($H_xSO_y$) and "nominally organic" ions in the HR-AMS, with minimal (approximately 0.5% of organic signal) organosulfur fragments. The OS fragmented to $H_xSO_y^+$ fragments with a pattern indistinguishable from inorganic sulfate aerosol, consistent with Liggio and Li (20). Further, no clear $T_v$ dependence in the $H_xSO_y^+$ fragmentation pattern was observed. One distinct organosulfur peak was observed, $CH_3SO_2^+$, accounting for $0.3 \pm 0.4\%$ of the S-containing ions signal at $T_v = 600$ °C (Table S1, Fig. 1*B*, and Fig. S7). Other organosulfur ions may have been present but could not be unequivocally quantified because of nearby large organic and/or $H_xSO_y$ peaks and the "ion sandwiching" described below for organonitrogen fragments. Including organosulfur fragments that were potentially influenced by S peaks and improved the residuals suggests that the organosulfur family accounts for a maximum of $1.0 \pm 0.8\%$ of the total S signal. No $C_xH_yS$ fragments (organosulfur without O) were observed. $CH_3SO_2^+$ has previously been considered a marker ion for MSA (29); however, this study suggests that this fragment is also indicative of OS and that the use of these markers to quantify either MSA or OS is limited to environments in which only one type of species is present. In the absence of MSA sources (i.e., away from marine aerosol), an upper estimate of OS could be obtained from the $CH_3SO_2^+$ fragment, similar to the method described below to estimate ON from organonitrogen fragments.

## Discussion

The results of these experiments suggest five approaches to quantifying ON in ambient AMS data, described in detail in *Materials and Methods*. They include (*I*) $NO_x^+$ fragmentation ratio, (*ii*) fragmentation to $HNO_3^+$ ions, (*iii*) fragmentation to $NO_x$-containing organic ions ($C_xH_yO_zN^+$), (*iv*) the $NH_4^+$ balance, and (*v*) the difference between total and inorganic $NO_3^-$. We applied the different methods for ON and OS estimation to ambient HR- AMS data acquired in Riverside, CA during the SOAR-1 campaign (30). OA was dominated by SOA (30), and the combination of high $NO_x$ and VOC concentrations should result in significant ON production. A comparison between the AMS $PM_1$ nitrate and ion chromatography (IC) $PM_{2.5}$ nitrate reveals agreement within the errors, which confirms that the majority of the AMS nitrate is inorganic (Fig. 2). However, given the uncertainty in both methods and the difference in size cuts, we cannot rule out an ON contribution of the order of 10% of the total nitrate. The AMS-only approaches provide additional constraints on ON estimates. In this study, the $NH_4^+$ required to achieve a charge balance with the measured AMS sulfate, nitrate, and chloride was predicted to be greater than measured $NH_4^+$, consistent with

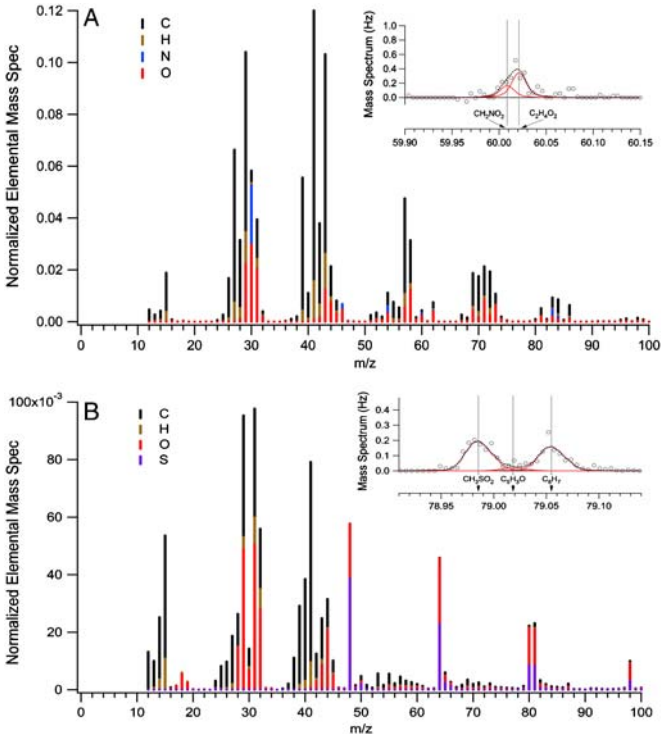


**Fig. 1.** (*a*) Mass spectrum of C, H, N and O in tetradecene-derived 2-hydroxynitrate standard taken with the HR-AMS ($T_v$ 600 °C). Data were taken and analyzed at high resolution, but are summed to unit mass resolution for display. Inset demonstrates resolution of organonitrogen peak from neighboring peaks at $m/z = 60$. (*b*) Mass spectrum of C, H, O, and S in the OS standard sampled with the HR-ToF-AMS ($T_v$ 600 °C). Inset shows high-resolution data of the dominant organosulfur peak ($CH_3SO_2^+$).

the presence of ON, OS, or some residual acidity ($H^+$). In this balance, OS was obtained from filter measurements as described below. This overprediction of $NH_4^+$ was linearly correlated ($r^2 = 0.70$) to $NO_3^-$, but uncorrelated with chloride or sulfate, consistent with ON. Assuming that the $NH_4^+$ overprediction is due to ON results in an upper limit for ON ("$ON_{NH4}$") of about 50% of the AMS nitrate. The correlation between $ON_{NH4}$ and AMS-$NO_3^-$ is poor ($r^2 = 0.32$), but has a slope of 0.08–0.22 depending on the regression assumptions, suggesting an alternate upper limit of ON of about 8–22% of the SOAR-1 total AMS nitrate. Applying the $NO_x^+$ fragmentation patterns described above, we calculate an upper limit of ON ("$ON_{NOx}$") about 50% of the observed AMS nitrate. Both $ON_{NH4}$ and $ON_{NOx}$ are upper limits and are larger than what the comparison of AMS to IC indicates, likely due to the assumptions that $NaNO_3$, $Ca(NO_3)_2$, and $H^+$ were not present, which would bias the estimates upward.

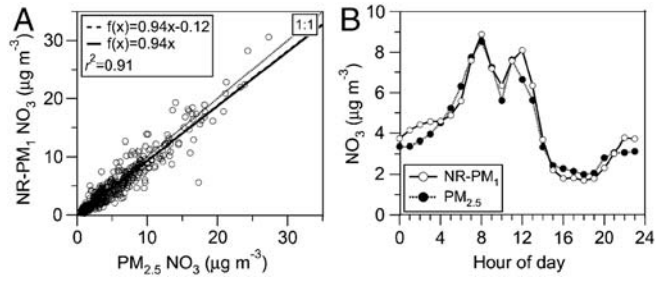


**Fig. 2.** (*a*) Intercomparison of AMS nitrate (y-axis) and IC nitrate (x-axis) during the SOAR-1 campaign in Riverside, CA. (*b*) Comparison of the diurnal cycles of both measurements.

The $ON_{CHON}$ calculation is hampered by the lack of resolvable $C_3H_4NO^+$ and $CH_4NO^+$ ions in the ambient data, suggesting that either the ON standards described above are not representative of ambient ON, or that ON contributions were minor during SOAR-1. Using the remaining three major CHON ions, we apply Eq. **2** to estimate $ON_{CHON}$, which is on average 4% (SD = 6%) of AMS nitrate. The assumptions of this approach are complicated by the presence of amines or other N-containing organics (31) that could lead to an $ON_{CHON}$ overestimate. Although ambient HR-AMS data were taken with $T_v = 350$ and 450 °C, the $HNO_3^+$ approach is of little use as the neighboring $CH_3SO^+$ ion ($m/z$ 62.9904) was approximately 10 to 100× larger than the $HNO_3^+$ ($m/z$ 62.9956) fragment, making quantitative assessment impossible. This test case highlights the difficulty of meeting the assumptions required to quantify ON with the HR-AMS. The fewest assumptions and most consistent results for the SOAR field dataset come from the $C_xH_yO_zN^+$ fragment and ammonium balance (nonzero intercept) approaches, which suggest contributions of ON to SOA on the order of 5–10% of the total AMS nitrate. If we assume that the organic fraction of the ON molecules has a molecular weight of 200 g/mol per $ONO_2$ group, then 0.8–1.6 μg $m^{-3}$ of the AMS OA (9.5–19% of the OA) may have ON functionalities.

Similar to ON, OS is fragmented into organic and sulfate components in the AMS. In contrast to ON, OS-sulfate are not sufficiently differently from $(NH_4)_2SO_4$ to enable quantification, or even to indicate the presence of OS from ratios of nominally inorganic sulfate fragments. The SOAR data do show clear $CH_3SO_2^+$ signals. If we assume this signal is from OS, we obtain an upper bound of approximately 45% contribution of OS to AMS sulfate. However, the Riverside site was impacted by marine aerosol, and MSA was observed by multiple instruments, which would heavily bias these OS estimates upward. Stone et al. detected approximately 6 nmol $m^{-3}$ particulate OS with molecular weight greater than 200 g/mol by (-)ESI-MS/MS (3). These results suggest approximately 12% of the AMS-$SO_4^{2-}$ could be due to OS, and are not inconsistent with the comparison with IC and the upper limit derived above, as well as the HR-AMS observations of $CH_2SO_3^+$ ions. If we assume that the organic fraction of the OS molecules has a molecular weight of 200 per OS group and take 12% of the AMS-$SO_4^{2-}$ to be OS, we estimate that 1.1 μg $m^{-3}$ AMS OA (12% of the AMS OA) have OS functionalities. Additional OS standards should be run in the HR-AMS to verify the robustness of the patterns reported here. Rural sites removed from marine air masses and other organosulfur aerosol sources will be more appropriate test cases for this OS estimation method. Intriguingly, this isoprene-derived OS standard was associated with $NH_4^+$, though not on an equimolar basis; the ammonium balance for the experiment shows that three $NH_4^+$ are predicted for every two observed. This implies that OS is not necessarily protonated, and can be negatively charged and associated with a counterion, consistent with particle-into-liquid sampler (PILS)/IC data collected from isoprene chamber experiments (32), and thus must be accounted for in the ammonium balance and in evaluations of aerosol acidity.

As described above, the elemental analysis of ambient OA with the HR-AMS typically excludes the nominally inorganic sulfate and nitrate signals. Assuming that 5–10% of the observed sulfate and nitrate signals are due to OS and ON and using the SOAR-1 data, we estimate that the impact on elemental analysis results of total ambient OA is substantial: The true O/C is typically underestimated by 10–20% (range 5–50%); N/C ratios are underestimated by a factor of 1.4–2 (range 1.2–3); and S/C ratios are underestimated by about an order of magnitude. Fig. 3 shows the comparison of the AMS elemental analysis results under different assumptions. The best agreement is obtained when it is assumed that the AMS quantitatively detects all oxygen in the molecule but completely misses the O in the $NO_2$ group

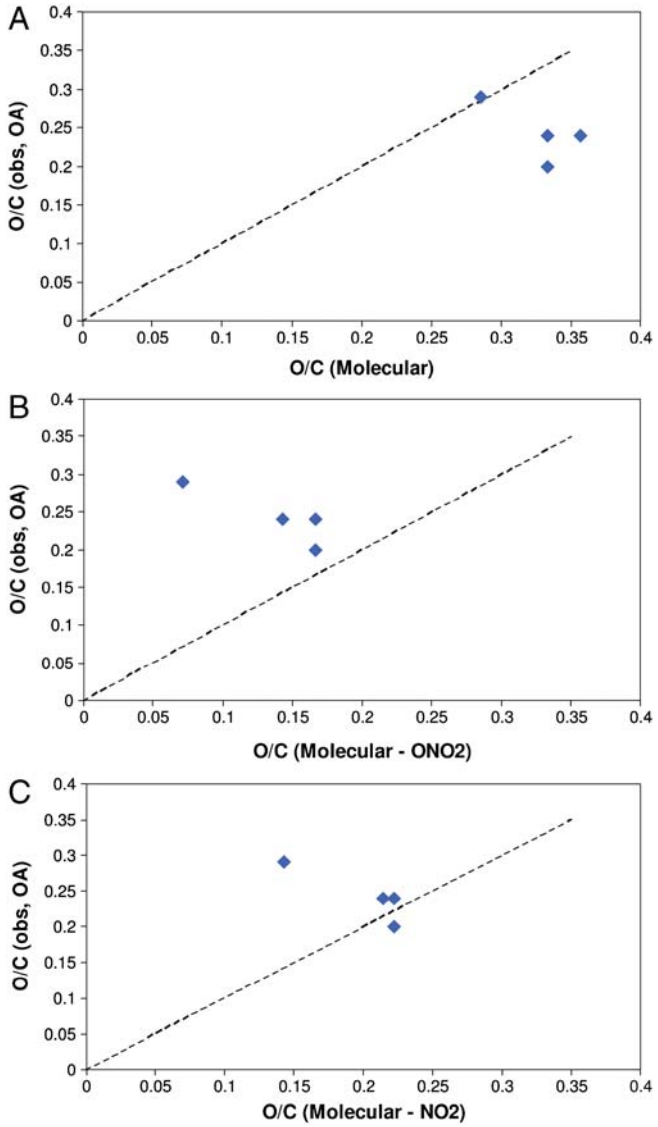


**Fig. 3.** The elemental analysis of OA from organic nitrate standards under three assumptions: (*a*) the AMS detects all oxygen in the ON in the organic component, (*b*) the AMS detects all oxygen in the ON but misses the O in the nitrate ($-ONO_2$) group, and (*c*) the AMS detects all oxygen in the ON but misses the O in the $NO_2$ group (but not the O bonded to the C atom). Dashed black lines show the 1:1 fit.

(but not the third O, which is bonded to a C atom), consistent with the discussion above.

This study has several implications for interpretation of field and laboratory data. First, the AMS measures ON (OS) primarily as organic and nitrate (sulfate) components. Thus, the AMS nitrate and sulfate from the standard AMS analysis software cannot be considered entirely inorganic species. Few organonitrogen ions are observed from ON, and many are difficult to accurately quantify because they are typically sandwiched between, or at tail edges of, large organic ions. Extreme care is needed in the fitting procedure, as otherwise large biases may result from false organic N peaks. The estimation of ON from SOAR-1 AMS data using different procedures highlight the challenges that arise due to the assumptions of each method, but give results that are roughly consistent with our current understanding of these species—namely that ON are likely present at levels of approximately 1 $\mu g\,m^{-3}$ and are 5–10% of the total nitrate mass, but do not dominate the total AMS nitrate signals. While the HR-AMS only provides an upper bound for OS, the data are not inconsistent with the estimate of Stone et al. resulting in approximately 10% of the total AMS sulfate signal being organic (3). Further, we have demonstrated that atmospheric ON and OS cause underestimations of the true O/C, N/C, and S/C ratios of OA by HR-AMS. Meaningful comparisons to models can be made by excluding the $NO_2$ (or $SO_3$) groups from the model elemental composition calculations. These results are not limited to the HR-AMS; because ON tend to thermally decompose to alkoxy and $NO_2$ radicals at moderate temperatures (33), other techniques that heat aerosols and/or that use energetic ionization before detection will suffer from the same limitations as described here for the HR-AMS, including aerosol mass spectrometers using thermal desorption, EI, or laser-ablation (34, 35). Our results demonstrate that OS decomposes during volatilization and/or ionization, similarly limiting the quantification ability of many aerosol detection techniques. Quantification of ON and OS with high time-resolution is essential for atmospheric chemistry studies, but most current state-of-the-art instrumentation has similar problems as the AMS for measuring these species. Although we studied only a handful of ON standards, they are derived from realistic experiments and cover a range of functionality consistent with what we expect in the urban atmosphere. Further, while ON fragmentation into an organic signal depends on the organic component, the C-O-$NO_2$ bond energies are consistent for all organic nitrates and are thus expected to fragment similarly. Additional ON and OS standards should be analyzed with the AMS to explore the robustness of the estimation techniques derived here, particularly the $ON_{CHON}$ approach, as should standards containing both ON and OS functionality, which have been observed in ambient aerosol (23). Alternate approaches for quantifying ON and OS more directly should be pursued including "softer" techniques, such as soft-ionization AMS, which may not fragment aerosol constituents to the extent of EI, or ESI-MS with an attempt at quantification (3). The TD-LIF approach is particularly promising as it quantifies the sum of gas and particle ON; to separate these two quantities, we propose that a denuder could be added to the TD-LIF, thereby removing gas-phase ON by diffusion and allowing separate analysis of particulate components.

## Materials and Methods

ON standards were synthesized in an environmental chamber by reacting oleic acid particles with $NO_3$ (OlA) (36) or 1-tetradecene vapor with $OH + NO_x$ (TD) (12). Synthesized particles were collected on Millipore filters [0.45 μm (OA) and 1.0 μm (TD) pore size, Fluoropore FHLP and FALP, 47 mm], which were then extracted in ethyl acetate and run through a high performance liquid chromatography (HPLC) system (Agilent 1100 Series) with UV-Vis diode array detector, aerosolized with a Collison atomizer, and sampled by HR-AMS. The HPLC separation method of ON into distinct peaks employed a water/methanol gradient elution: 50% methanol for 10 min increasing to 100% over 50 min. Each chromatographic peak is a pure standard that has been previously characterized (12). Standards derived from OlA included carbonylnitrate isomers (OlA-CN), hydroxynitrate isomers (OlA-HN), and OlA-CN + OlA-HN oligomers (OlA-olig), while those derived from TD included dihydroxynitrate isomers (TD-DHN), a 2-hydroxy-1-nitrate (TD-2OH-HN), and a 1-hydroxy-2-nitrate (TD-1OH-HN). Note that all OlA-CN and OlA-HN compounds have a carboxyl group from the oleic acid parent. Standards were sampled by the HR-AMS at least three times each, and at each of three AMS $T_v$ (200, 400, and 600 °C). An OS standard, previously characterized as a trihydroxy sulfate ester of isoprene ($C_5H_{12}O_7S$) (23), was obtained from high-volume filter sampling conducted at Jefferson Street in downtown Atlanta, GA during summer 2004 (23). The sample was isolated by HPLC separation in acetonitrile before HR-AMS detection.

An Aerodyne HR-ToF-AMS (HR-AMS for short), described in detail previously (37), was used for all analyses. All experiments were performed in the highest resolution mode ("W-mode", $m/\Delta m \sim 5,000$) to optimize peak separation. Data analysis procedures for the HR-AMS have been previously described in detail (28, 37), and give quantitative data on individual ions and elemental ratios. Briefly, the ion time-of-flight is calibrated to mass to charge ($m/z$) ratios through known $m/z$ peaks, and mathematical expressions for the average ion peak width and shape are derived. These

parameters are then used to fit a user-chosen list of ion fragments. The contribution of background ions is accounted for by subtracting a "closed" spectrum acquired when the particle and gas beam are blocked and do not reach the vaporizer/ionizer stage. Additionally, we subtracted a background particle and solvent signal for each of the ON standards, using the average spectrum of the chromatographic baseline. The background total signal was at least three orders of magnitude smaller than the chromatography peak signals used in this analysis.

We chose the ion fragment list for fitting conservatively: Ions that were not clearly present in any of the standards (i.e., excluding the ion from the fit list did not significantly alter the residual, or that including the ion may have improved the residual but altered the shape of the calculated mass spectrum such that it was inconsistent with the observed spectrum) were excluded, thus avoiding spurious signals. A second fragment list was compiled for comparison purposes, which included all viable combinations of $C_{1-8}H_yO_{0-3}N_{0-2}$. Note that no $C_xH_yN_p$ fragments were included in the standard fragment list, but were included in the extended version. We assign every ion fragment to a "family" of similar atom combinations; the relevant families in this experiment are the $C_xH_yO_z$, $C_xH_yO_zN_p$, $C_xH_y$, and $C_xH_yN_p$ combinations, which collectively comprise the organic signal; the $NH_y$ family (ammonium signal), the $H_xSO_y$ (sulfate signal) and the $H_xN_yO_z$ family (nitrate signal).

**Approaches to Quantifying ON with the HR-AMS.** ***$NO_x^+$ ratio ($ON_{NOx}$).*** The nitrate portion of inorganic and organic nitrates primarily fragments to $NO^+ + NO_2^+$. Nitrate fragmentation, and thus observed $NO^+/NO_2^+$ ratio ($NO_x^+$ ratio), is different for ON vs. $NH_4NO_3$ and may allow ON quantification. Fry et al. (1) report a $NO_x^+$ ratio of approximately 10/1 from the unit mass resolution $m/z$ 30 and 46 peaks of aerosol derived from $NO_3 + \beta$-pinene reactions, while Bruns et al. report $NO_x^+$ ratios of 10–15 for aerosol derived from various $NO_3$ + monoterpene reactions and approximately 5 for $NO_3$ + isoprene reactions (13). Fry et al. found this ratio to be much larger than that observed for $NH_4NO_3$ (2.7) and independent of $T_v$, though unit mass resolution was used, and the $m/z$ 30 signal was likely impacted by organic fragments. Bruns et al. also found the organic ratios to be higher than that of $NH_4NO_3$ (2.4). We note that the $NO_x^+$ ratio can depend on the specific instrument, but relative trends should be comparable between instruments. We calculated the ratio from HR mass spectra to avoid possible interferences. The average $NO_x^+$ ratio for all the ON standards analyzed at a $T_v$ of 600 °C was $3.5 \pm 0.3$ (errors associated with average values are standard errors of the mean unless otherwise stated) with a minimum of $1.8 \pm 0.5$ for a tetradecene-derived hydroxynitrate and a maximum of $4.6 \pm 0.2$ for oleic acid-derived hydroxynitrates. There was no clear effect of $T_v$ on the ratio. The average $NO_x^+$ ratio of 3.5 is similar to the value of 3.0 measured for $NO_2$ (38), suggesting that a large fraction of $RONO_2$ decomposes on the vaporizer to $RO + NO_2$ and that then $NO_2$ is ionized (33). By contrast, ratios for $HNO_3$ (0.5) (39) and $NH_4NO_3$ ($1.5 \pm 0.1$ for the instrument used in this experiment) are much smaller.

Because $NH_4NO_3$ and ON give very different average $NO_x^+$ ratios ($R_{NH4NO3}$ and $R_{ON}$), the observed ambient ratio, $R_{obs}$, could potentially be used to estimate the fraction of the total nitrate signal due to ON ($x$), with an associated uncertainty ($\Delta x$, *SI Text*) derived from the uncertainties in calibration and observed ratios ($S_R$):

$$x = \frac{(R_{obs} - R_{NH_4NO_3})(1 + R_{ON})}{(R_{ON} - R_{NH_4NO_3})(1 + R_{obs})} \quad [1]$$

For example, an observed $NO_x^+$ ratio of $2.0 \pm 0.2$ results in an ON fraction of $0.4 \pm 0.2$. There are four important caveats for this approach, however. First, as fragmentation depends on instrument tuning, $NH_4NO_3$ standards need to be run in the field (which is typically done as part of AMS calibrations) while running ON standards would also be useful. Second, ON need to be a substantial fraction of total AMS nitrate in order to be adequately resolved by this approach. Third, inorganic nitrates such as $NaNO_3$ and $Ca(NO_3)_2$ can also give large $NO_x^+$ ratios and were postulated to cause elevated $NO_x^+$ ratios (5 to 7) at a coastal site in California during the Intercontinental Transport and Chemical Transformation (ITCT) campaign (40). Thus, use of the $NO_x^+$ ratio to quantify ON is limited to areas where mineral and sea-salt nitrates and other species (e.g., inorganic or organic nitrites, nitro-organics, and amides) do not contribute significantly to $NO_x^+$ fragments. Fourth, this approach assumes that fragmentation patterns of the multifunctional ON standards analyzed here are representative of ambient ON.

***$HNO_3/NO_x$ ratios ($ON_{HNO3}$).*** Inorganic oxidized nitrogen ions other than $NO_x^+$ are detected in different fractions for various nitrates. $HNO_3^+$ ions ($m/z$ 62.9956) are far enough from the left edge of the neighboring $C_5H_3^+$ ion ($m/z$ 63.0235) to be clearly resolved. $HNO_3^+$ is observed in both $NH_4NO_3$ and ON standards under standard HR-AMS operating conditions, accounting for a small fraction of N-containing ON peaks (<0.02%). Moreover, the $HNO_3^+/NO_x^+$ ratio in the $NH_4NO_3$ spectrum shows a linear temperature dependence, with $HNO_3^+$ accounting for 0,0.38, and 0.68% of the inorganic nitrate N-ions at $T_v = 600$, 400, and 200 °C. The temperature dependence of $HNO_3^+/NO_x^+$ in ON is less clear because the $HNO_3^+$ ions are small and have larger uncertainties at 200 °C than at 600 °C due to less fragmentation to $HNO_3^+$ coupled with high neighboring organic ions in the standards. Although the signals are too uncertain at very low and very high $T_v$ to discern trends, $HNO_3^+$ is a clear ON peak at 400 °C, which provides a contrast with $NH_4NO_3$. We use the same approach and uncertainty analysis as for the $NO_x^+$ ratios to calculate the relative contribution of ON to total AMS nitrate from the $HNO_3^+/NO_x^+$ at 400 °C. For example, an observed ratio of 0.0027 (30% relative error) gives an ON contribution to total nitrate of $0.3 \pm 0.4$. The uncertainty is larger in this approach than the previous approach because of greater uncertainties (30–40%) in the $HNO_3^+$ signal. As outlined above, the fragmentation pattern depends on instrument tuning, and thus $HNO_3^+/NO_x^+$ ratios should be determined in the field for both ON and $NH_4NO_3$ standards at 400 °C. This approach is also sensitive to the presence of other types of species that can produce these ions, as it assumes that $NH_4NO_3$ and ON are the only source of $HNO_3^+$ and $NO_x^+$ ions.

***$C_xH_yO_zN^+$ fragments ($ON_{CHON}$).*** While individual ON standards have different major ions and patterns, we can use the sum of the signals of the five major $C_xH_yO_zN^+$ ions, $\Sigma CHON = CH_4NO^+ + C_2H_5NO^+ + C_3H_4NO^+ + CH_2NO_3^+ + CH_2NO_2^+$, to quantify ON, assuming that ON are the only source of these ions, that our set of standards is representative of ambient mixtures of atmospheric ON, and that the ions can be adequately resolved from neighboring organic ions in ambient aerosol. We note that the formation of some of these ions from our ON standards would require complex rearrangements. ΣCHON accounts for $5 \pm 2\%$ of the total oxidized N signal ($C_xH_yO_zN^+ + H_xNO_y^+$) in the standards analyzed here. The ambient ON signal calculated using this fraction ($R_{CHON} = 0.045$) and observed ΣCHON, with uncertainties calculated by error propagation, is

$$ON = \Sigma CHON_{observed}/R_{CHON} \quad [2]$$

For example, for the instrument described in this experiment ($R_{CHON} = 0.045$, $\Delta R_{CHON} = 0.018$), a value of $\Sigma CHON_{observed} = 0.020 \pm 0.004\ \mu g\,m^{-3}$ corresponds to $0.5 \pm 0.2\ \mu g\,m^{-3}$ ON. Imidazoles are likely interferences in this analysis: They are formed during glyoxal uptake on ammonium sulfate, amines, and amino acids, and while they mostly form $C_xH_yN^+$ ions, they can produce $C_2H_3NO^+$, $C_3H_2NO^+$, and $CH_4NO^+$ ions in the HR-AMS (41). Thus, this approach may be inappropriate if reduced N ions were observed, indicating the presence of imidazoles or other non-ON organic N.

***Ammonium balance ($ON_{NH4}$).*** The $NH_4^+$ mass required to balance the inorganic anions ($SO_4^{2-}$, $Cl^-$, $NO_3^-$) should match the observed $NH_4^+$ in ambient aerosol when gas-phase ammonia is abundant. When this calculation is done with AMS data, low measured/predicted $NH_4^+$ is generally interpreted as due to acidic aerosols with excess $H_2SO_4$ or $NH_4HSO_4$ (24). However this observation could also be due to the presence of ON and/or OS, as these species increase the nominally inorganic AMS nitrate and sulfate, respectively, and thus affect the observed $NH_4^+$ balance. The discrepancy between measured and calculated $NH_4^+$ may provide an alternate procedure for placing bounds on ambient ON with the AMS in the absence of nominally ammonium (i.e., amines), sulfate (i.e., OS, MSA) or nitrate [i.e., $NaNO_3$, $Ca(NO_3)_2$], fragments.

***Difference between total and inorganic $NO_3^-$.*** Subtracting known inorganic $NO_3^-$ (e.g., IC measurements) from AMS nitrate is a fifth possibility for quantifying ON. However, this approach requires that both techniques measure the same air masses and sample with identical size cuts. Perhaps more challenging is the requirement that the two instruments both demonstrate a high level of accuracy and precision and are cross-calibrated with identical standards. For example, at Trinidad Head, CA during the ITCT campaign, the difference between AMS-$NO_3^-$ and PILS-IC nitrate was consistent with ON (40) and would account for <2% of $NO_y$, but up to half of the AMS-$NO_3^-$ (40); however, the two relevant instruments were not cross-calibrated, and it is unlikely they had identical inlet losses or size cuts.

**Potential Overestimation of Organonitrogen Ions.** In the analysis presented here, we excluded any ions that were not clearly identifiable given the

limited resolution of the HR-AMS, providing a conservative, lower-limit estimate of organonitrogen fragments. A key reason for excluding unnecessary ions in the fitting routine is the bias toward overestimation of organonitrogen fragments. $C_xH_yN_p^+$ ions are typically sandwiched between large $CH^+$ and $CHO^+$ ions in HR-AMS spectra, and can easily provide spurious peaks. The HR-AMS peak fitting routines (37) produces either a positive or zero fit to chosen ions, but no negative fits, so small errors in the *m/z*-ion time-of-flight calibration, or peak width and shape estimates will result in either no effect or a positive artifact in spurious ions at the expense of real ions. Further, the more ions included in the fits, the better the fits will necessarily be because more degrees of freedom are allowed, whether or not the ions are actually present. The detection of $C_xH_yN_p^+$ ions from ON in the AMS would be surprising because it would involve rearrangements that somehow break the C-$ONO_2$ bond, remove all the O atoms from $NO_3$, and then form a C-N bond. This is highly unlikely, particularly when compared to straightforward mechanistic pathways to $C_xH_yO_zN_p^+$ ions. Because no evidence for $C_xH_yN_p^+$ ions was observed (i.e., no improvement in the residuals between measured and fitted mass spectra if these ions were fitted), this dataset was used to investigate the effect of including extra, spurious ions in the fitting procedure. With the identical fitting parameters, an additional 383 peaks were fit to the AMS mass spectra of oleic acid-derived ON standards, including all $C_xH_yN_p^+$ and $C_xH_yO_zN_p^+$ as well as ions that were not expected to be present in the experiment but are typically included in ambient data analysis. Inclusion of additional $C_xH_yO_zN_p^+$ ions caused the fraction of ON-N recovered in $C_xH_yO_zN_p^+$ ions to increase from 5 to 20–43%. The upper limit is due mostly to the analysis procedure fitting $C_xH_yN_p^+$ ions in place of neighboring $C_xH_yO_z^+$ ions. This effect, potentially due to minute shifts in the *m/z* calibration, both overestimates N and underestimates O in the sample. These results highlight the need for high-quality *m/z* calibrations and peak width/shape parameters when attempting to quantify minor fragments in AMS spectra, and also the danger of blindly fitting ions without strong evidence that they exist. Higher mass resolution than is achieved in the current HR-AMS (approximately 5,000) is highly desirable to reduce these errors and uncertainties. The relevance of this limitation and potential overestimation is not limited to HR-AMS instrumentation, but to any high-resolution mass spectral analysis using the same approach, including chemical ionization or proton-transfer reaction mass spectrometry.

**ACKNOWLEDGMENTS.** This study was funded by National Science Foundation Grants ATM0449815 and 0650061, National Oceanic and Atmospheric Administration Grant NA08OAR4310565, and Department of Energy Biological and Environmental Research/Atmospheric Science Program Grant DEFG0208ER64627. We thank D. Eatough (Brigham Young University) for the ion chromatography data. We thank J. Kroll, B. Finlayson-Pitts, and two anonymous reviewers for useful suggestions.

1. Fry JL, et al. (2009) Organic nitrate and secondary organic aerosol yield from $NO_3$ oxidation of β-pinene evaluated using a gas-phase kinetics/aerosol partitioning model. *Atmos Chem Phys* 9:1431–1449.
2. Ng NL, et al. (2008) Secondary organic aerosol (SOA) formation from reaction of isoprene with nitrate radicals ($NO_3$). *Atmos Chem Phys* 8:4117–4140.
3. Stone EA, Hedman CJ, Sheesley RJ, Shafer MM, Schauer JJ (2009) Investigating the chemical nature of humic-like substances (HULIS) in North American atmospheric aerosols by liquid chromatography tandem mass spectrometry. *Atmos Environ* 43:4205–4213.
4. Surratt JD, et al. (2007) Evidence for organosulfates in secondary organic aerosol. *Environ Sci Technol* 41:517–527.
5. Day DA, et al. (2003) On alkyl nitrates, $O_3$, and the "missing $NO_y$". *J Geophys Res* 108:4501 doi: 10.1029/2003JD003685.
6. Perring AE, et al. (2009) Airborne observations of total $RONO_2$: New constraints on the yield and lifetime of isoprene nitrates. *Atmos Chem Phys* 9:1451–1463.
7. Rosen RS, et al. (2004) Observations of total alkyl nitrates during Texas Air Quality Study 2000: Implications for $O_3$ and alkyl nitrate photochemistry. *J Geophys Res* 109:D07303 doi: 10.1029/2003JD004227.
8. Bertman SB, et al. (1995) Evolution of alkyl nitrates with air-mass age. *J Geophys Res* 100:22805–22813.
9. Atkinson R, Arey J (2003) Atmospheric degradation of volatile organic compounds. *Chem Rev* 103:4605–4638.
10. Camredon M, Aumont B, Lee-Taylor J, Madronich S (2007) The SOA/VOC/$NO_x$ system: An explicit model of secondary organic aerosol formation. *Atmos Chem Phys* 7:5599–5610.
11. Lim YB, Ziemann PJ (2009) Chemistry of secondary organic aerosol formation from OH radical-initiated reactions of linear, branched, and cyclic alkanes in the presence of $NO_x$. *Aerosol Sci Technol* 43:604–619.
12. Matsunaga A, Ziemann PJ (2009) Yields of β-hydroxynitrates and dihydroxynitrates in aerosol formed from OH radical-initiated reactions of linear alkenes in the presence of $NO_x$. *J Phys Chem A* 113:599–606.
13. Bruns EA, et al. (2010) Comparison of FTIR and Particle Mass Spectrometry for the Measurement of Particulate Organic Nitrates. *Environ Sci Technol* 44:1056–1061.
14. Garnes LA, Allen DT (2002) Size distributions of organonitrates in ambient aerosol collected in Houston, Texas. *Aerosol Sci Technol* 36:983–992.
15. Weathers W (2004) Comments on "Size distribution of organonitrates in ambient aerosol collected in Houston, Texas". *Aerosol Sci Technol* 38:782–786.
16. Gilardoni S, et al. (2009) Characterization of organic ambient aerosol during MIRAGE 2006 on three platforms. *Atmos Chem Phys* 9:5417–5432.
17. Nielsen T, Egelov AH, Granby K, Skov H (1995) Observations on particulate organic nitrates and unidentified components of $NO_y$. *Atmos Environ* 29:1757–1769.
18. Day DA, Wooldridge PJ, Dillon MB, Thornton JA, Cohen RC (2002) A thermal dissociation laser-induced fluorescence instrument for in situ detection of $NO_2$, peroxy nitrates, alkyl nitrates, and $HNO_3$. *J Geophys Res* 107:4046 doi: 10.1029/2001JD000779.
19. Lin M, Walker J, Geron C, Khlystov A (2009) Organic nitrogen in $PM_{2.5}$ aerosol at a forest site in the Southeast US. *Atmos Chem Phys Discuss* 9:17157–17181.
20. Liggio J, Li SM (2006) Organosulfate formation during the uptake of pinonaldehyde on acidic sulfate aerosols. *Geophys Res Lett* 33:L13808 doi: 10.1029/2006GL026079.
21. Altieri KE, Turpin BJ, Seitzinger SP (2009) Oligomers, organosulfates, and nitrooxy organosulfates in rainwater identified by ultra-high resolution electrospray ionization FT-ICR mass spectrometry. *Atmos Chem Phys* 9:2533–2542.
22. Lukács H, et al. (2009) Quantitative assessment of organosulfates in size-segregated rural fine aerosol. *Atmos Chem Phys* 9:231–238.
23. Surratt JD, et al. (2008) Organosulfate formation in biogenic secondary organic aerosol. *J Phys Chem A* 112:8345–8378.
24. Zhang Q, Jimenez JL, Worsnop DR, Canagaratna M (2007) A case study of urban particle acidity and its influence on secondary organic aerosol. *Environ Sci Technol* 41:3213–3219.
25. Zhang Q, et al. (2007) Ubiquity and dominance of oxygenated species in organic aerosols in anthropogenically-influenced Northern Hemisphere midlatitudes. *Geophys Res Lett* 34:L13801 doi: 10.1029/2007GL029979.
26. Ulbrich IM, Canagaratna MR, Zhang Q, Worsnop DR, Jimenez JL (2009) Interpretation of organic components from positive matrix factorization of aerosol mass spectrometric data. *Atmos Chem Phys* 9:2891–2918.
27. Aiken AC, DeCarlo PF, Jimenez JL (2007) Elemental analysis of organic species with electron ionization high-resolution mass spectrometry. *Anal Chem* 79:8350–8358.
28. Aiken AC, et al. (2008) O/C and OM/OC ratios of primary, secondary, and ambient organic aerosols with high-resolution time-of-flight aerosol mass spectrometry. *Environ Sci Technol* 42:4478–4485.
29. Zorn SR, Drewnick F, Schott M, Hoffmann T, Borrmann S (2008) Characterization of the South Atlantic marine boundary layer aerosol using an aerodyne aerosol mass spectrometer. *Atmos Chem Phys* 8:4711–4728.
30. Docherty KS, et al. (2008) Apportionment of primary and secondary organic aerosols in Southern California during the 2005 Study of Organic Aerosols in Riverside (SOAR-1). *Environ Sci Technol* 42:7655–7662.
31. Huffman JA, et al. (2009) Chemically-resolved volatility measurements of organic aerosol from different sources. *Environ Sci Technol* 43:5351–5357.
32. Surratt JD, et al. (2007) Effect of acidity on secondary organic aerosol formation from isoprene. *Environ Sci Technol* 41:5363–5369.
33. Francisco MA, Krylowski J (2005) Chemistry of organic nitrates: Thermal chemistry of linear and branched organic nitrates. *Ind Eng Chem Res* 44:5439–5446.
34. Murphy DM (2007) The design of single particle laser mass spectrometers. *Mass Spectrom Rev* 26:150–165.
35. Hung HM, Katrib Y, Martin ST (2005) Products and mechanisms of the reaction of oleic acid with ozone and nitrate radical. *J Phys Chem A* 109:4517–4530.
36. Docherty K, Ziemann P (2006) Reaction of oleic acid particles with NO3 radicals: Products, mechanism, and implications for radical-initiated organic aerosol oxidation. *J Phys Chem A* 110:3567–3577.
37. DeCarlo PF, et al. (2006) Field-deployable, high-resolution, time-of-flight aerosol mass spectrometer. *Anal Chem* 78:8281–8289.
38. Lopez J, Tarnovsky V, Gutkin KKB (2003) Electron-impact ionization of NO, $NO_2$, and $N_2O$. *Int J Mass Spectrom* 225:25–37.
39. O'Connor C, Jones N, Price S (1997) Electron-impact ionization of nitric acid. *Int J Mass Spectrom* 163:131–139.
40. Allan JD, et al. (2004) Submicron aerosol composition at Trinidad Head, California, during ITCT 2K2: Its relationship with gas phase volatile organic carbon and assessment of instrument performance. *J Geophys Res* 109:D23S24 doi: 10.1029/2003JD004208.
41. De Haan DO, et al. (2009) Secondary Organic Aerosol-Forming Reactions of Glyoxal with Amino Acids. *Environ Sci Technol* 43:2818–2824.

# Supporting Information

## Farmer et al. 10.1073/pnas.0912340107

### SI Text

**Error Analysis for ON Estimation Methods.** If we take the observed $NO_x^+$ ratio to be the combination of $NO_x^+$ ions from $NH_4NO_3$ and organonitrate (ON), and the fractional contribution of ON ions to $NO_x^+$ to be proportional to the fractional contribution of ON to total $NO_{3^-}$,

$$x = \frac{NO_{ON} + NO_{2,ON}}{NO_{obs} + NO_{2,obs}}, \quad [S1]$$

$$R_{obs} = \frac{NO_{obs}}{NO_{2,obs}} = \frac{NO_{NH_4NO_3} + NO_{ON}}{NO_{2,NH_4NO_3} + NO_{2,ON}}, \quad [S2a]$$

$$R_{NH_4NO_3} = \frac{NO_{NH_4NO_3}}{NO_{2,NH_4NO_3}}, \quad [S2b]$$

$$R_{ON} = \frac{NO_{ON}}{NO_{2,ON}}, \quad [S2c]$$

Combining Eq. S2a–S2c,

$$R_{obs} = \frac{R_{NH_4NO_3}NO_{2,NH_4NO_3} + R_{ON}NO_{2,ON}}{NO_{2,NH_4NO_3} + NO_{2,ON}}. \quad [S3]$$

Taking $NO_{2,NH4NO3} = NO_{2,obs} - NO_{2,ON}$, Eq **S3** can be rewritten,

$$R_{obs}(NO_{2,obs}) = R_{NH_4NO_3}(NO_{2,obs} - NO_{2,ON}) + R_{ON}NO_{2,ON}, \quad [S4]$$

$$NO_{2,obs}(R_{obs} - R_{NH_4NO_3}) = NO_{2,ON}(R_{ON} - R_{NH_4NO_3}). \quad [S5]$$

Thus, the $NO_2^+$ derived from ON in the high-resolution version of the aerosol mass spectrometer (HR-AMS) is

$$NO_{2,ON} = \frac{NO_{2,obs}(R_{obs} - R_{NH_4NO_3})}{(R_{ON} - R_{NH_4NO_3})}. \quad [S6]$$

From our definition of $R_{ON}$,

$$NO_{ON} = \frac{R_{ON}NO_{2,obs}(R_{obs} - R_{NH_4NO_3})}{(R_{ON} - R_{NH_4NO_3})}. \quad [S7]$$

Eq. **S1** can then be rewritten,

$$x = \frac{(R_{ON} + 1)NO_{2,obs}(R_{obs} - R_{NH_4NO_3})/(R_{ON} - R_{NH_4NO_3})}{(NO_{obs} + NO_{2,obs})}, \quad [S8]$$

$$x = \frac{(R_{ON} + 1)NO_{2,obs}(R_{obs} - R_{NH_4NO_3})}{(R_{ON} - R_{NH_4NO_3})(R_{obs}NO_{2,obs} + NO_{2,obs})}, \quad [S9]$$

$$x = \frac{(R_{obs} - R_{NH_4NO_3})(1 + R_{ON})}{(R_{ON} - R_{NH_4NO_3})(1 + R_{obs})}. \quad [S10]$$

By error propagation from Eq. **S10** (Eq. **1** in manuscript) and Eq. **2**, the uncertainty associated with $ON_{NOx}$ ($\Delta_x$) and $ON_{CHON}$ ($\Delta_{ON}$) are

$$\Delta_x = x * \sqrt{\frac{S_{R_{obs}}^2 + S_{R_{NH_4NO_3}}^2}{(R_{obs} - R_{NH_4NO_3})^2} + \frac{S_{R_{ON}}^2 + S_{R_{NH_4NO_3}}^2}{(R_{ON} - R_{NH_4NO_3})^2} + \left(\frac{S_{R_{ON}}}{R_{ON}}\right)^2 + \left(\frac{S_{R_{obs}}}{R_{obs}}\right)^2}, \quad [S11]$$

$$\Delta_{ON} = \frac{\sum CHON_{major,obs}}{R_{CHON_{major}}} * \sqrt{\left(\frac{\Delta(\Sigma CHON_{major,obs})}{\Sigma CHON_{major,obs}}\right)^2 + \left(\frac{\Delta R_{CHON_{major}}}{R_{CHON_{major}}}\right)^2}. \quad [S12]$$

1. Hogrefe O, Drewnick F, Lala GG, Schwab JJ, Demerjian KL (2004) Development, operation and applications of an aerosol generation, calibration and research facility. *Aerosol Sci Technol* 38:196–214.

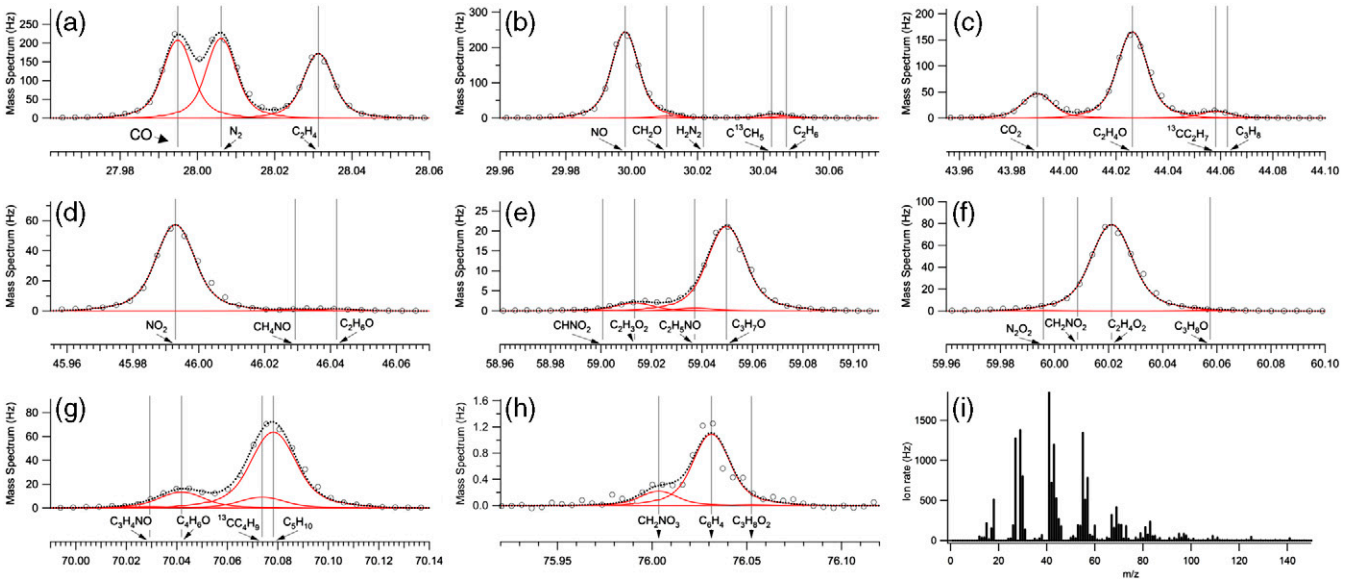


**Fig. S1.** High-resolution mass spectra (*a–h*) at dominant N-containing $m/z$ ratios, along with $m/z$ 28 and 44, for the oleic acid-derived hydroxynitrate (OlA-HN), taken at $T_v = 600\,°C$. The complete mass spectrum (*i*) is presented at unit mass resolution.

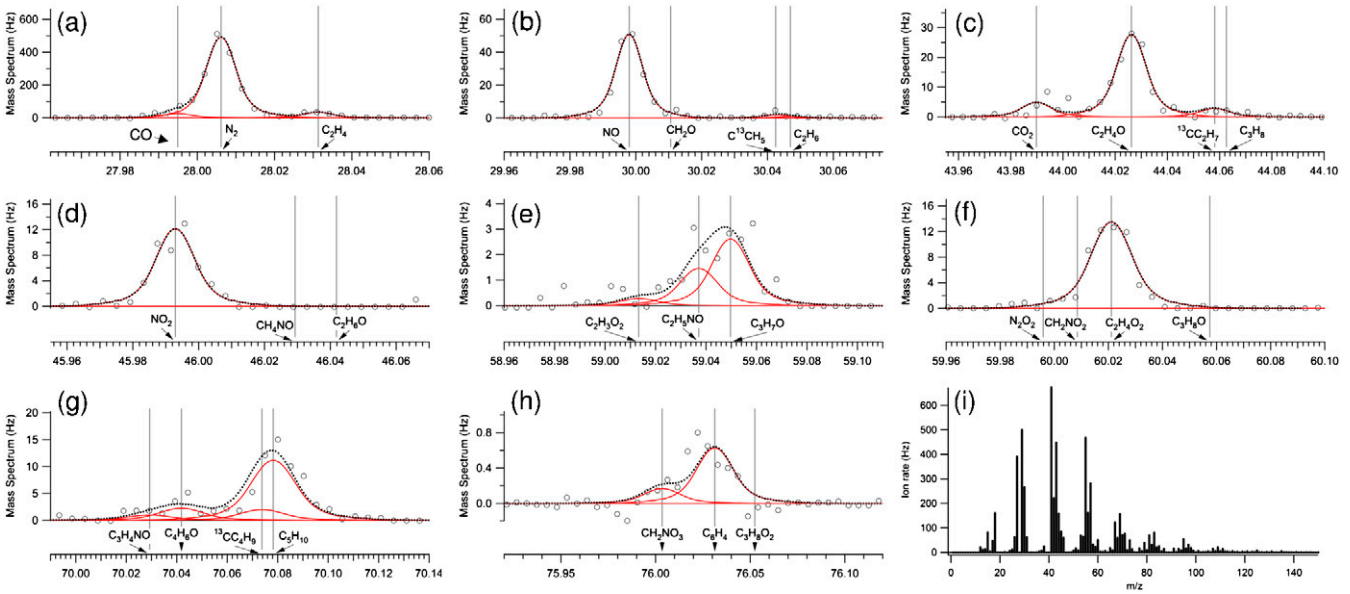


**Fig. S2.** High-resolution mass spectra (*a–h*) at dominant N-containing $m/z$ ratios, along with $m/z$ 28 and 44, for the oleic acid-derived carbonylnitrate (OlA-CN), taken at $T_v = 600\,°C$. The complete mass spectrum (*i*) is presented at unit mass resolution.

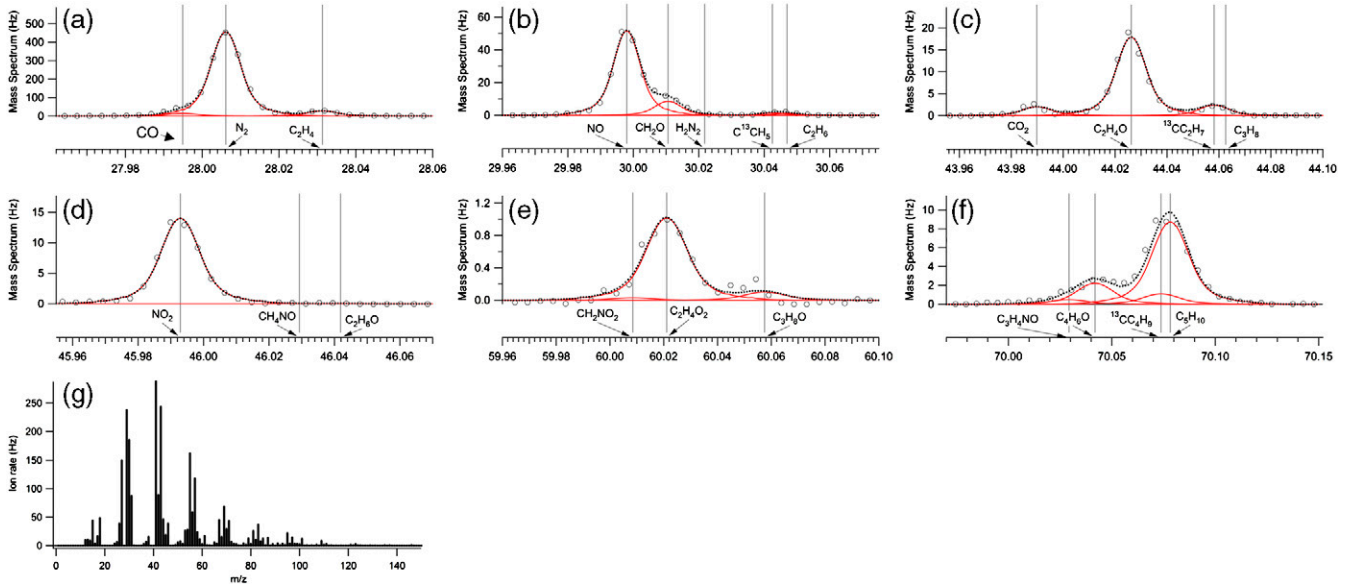


**Fig. S3.** High-resolution mass spectra (*a–f*) at dominant N-containing $m/z$ ratios, along with $m/z$ 28 and 44, for the tetradecene-derived dihydroxynitrate (TD-DHN), taken at $T_v = 600$ °C. The complete mass spectrum (*g*) is presented at unit mass resolution.

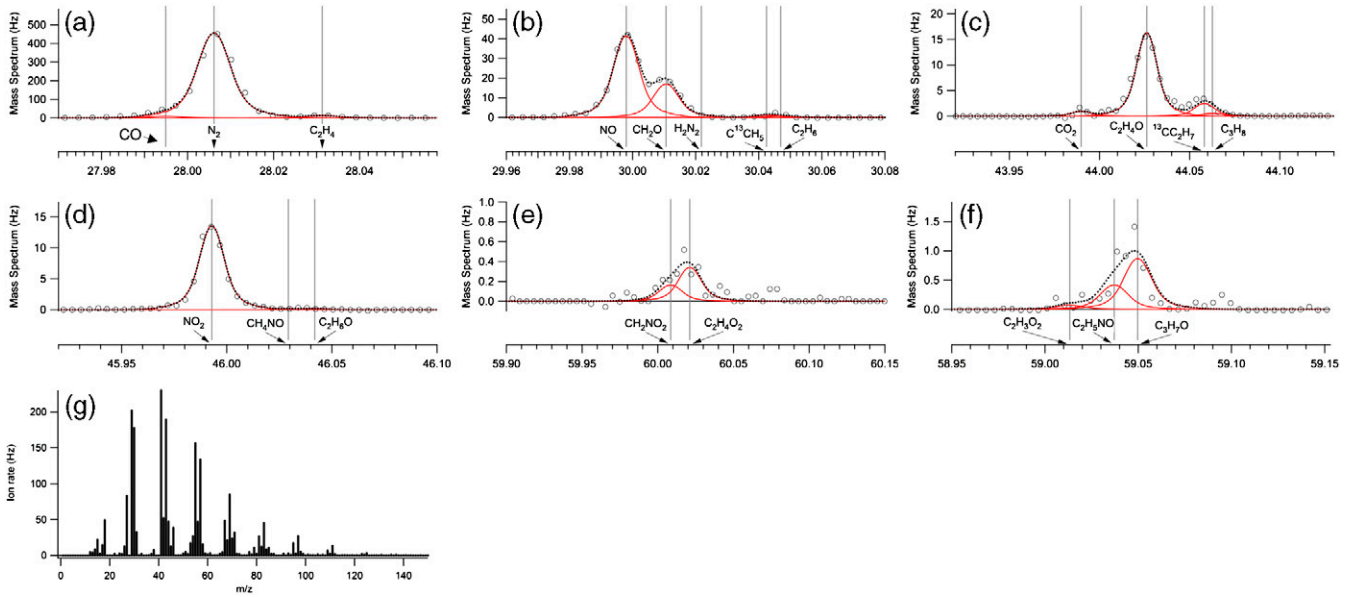


**Fig. S4.** High-resolution mass spectra (*a–f*) at dominant N-containing $m/z$ ratios, along with $m/z$ 28 and 44, for the tetradecene-derived 2-hydroxynitrate (TD-2OH-HN), taken at $T_v = 600$ °C. The complete mass spectrum (*g*) is presented at unit mass resolution.

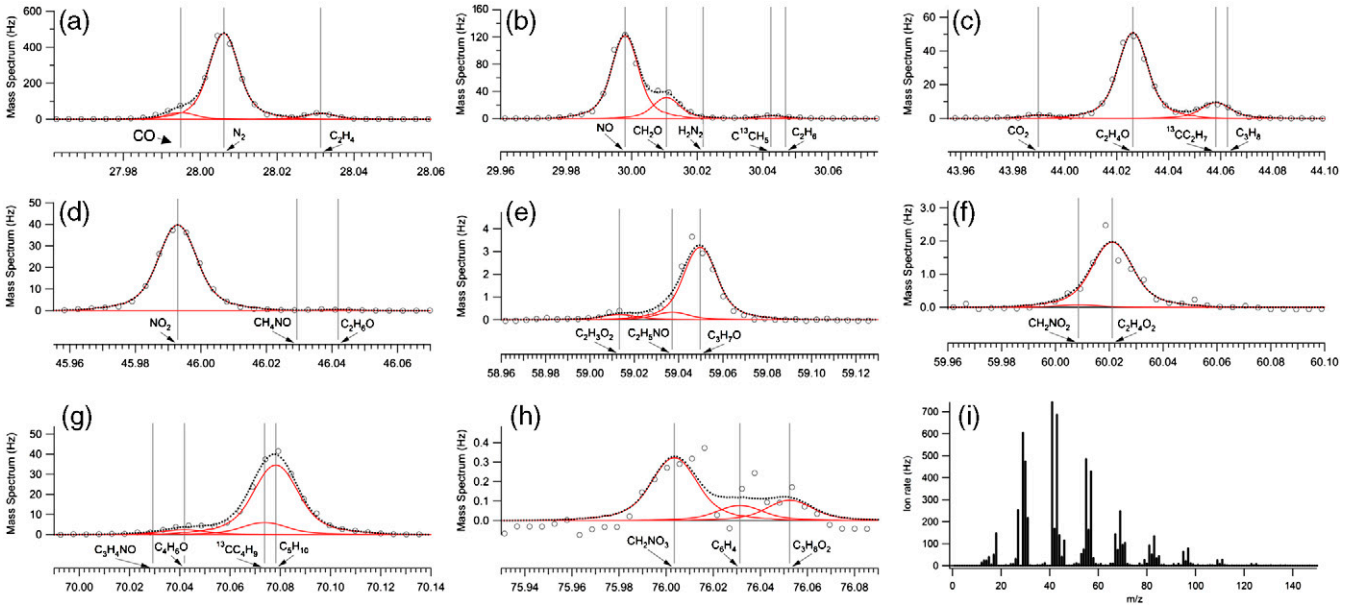


**Fig. S5.** High-resolution mass spectra (*a*–*h*) at dominant N-containing $m/z$ ratios, along with $m/z$ 28 and 44, for the tetradecene-derived 1-hydroxynitrate (TD-1OH-HN), taken at $T_v = 600$ °C. The complete mass spectrum (*i*) is presented at unit mass resolution.

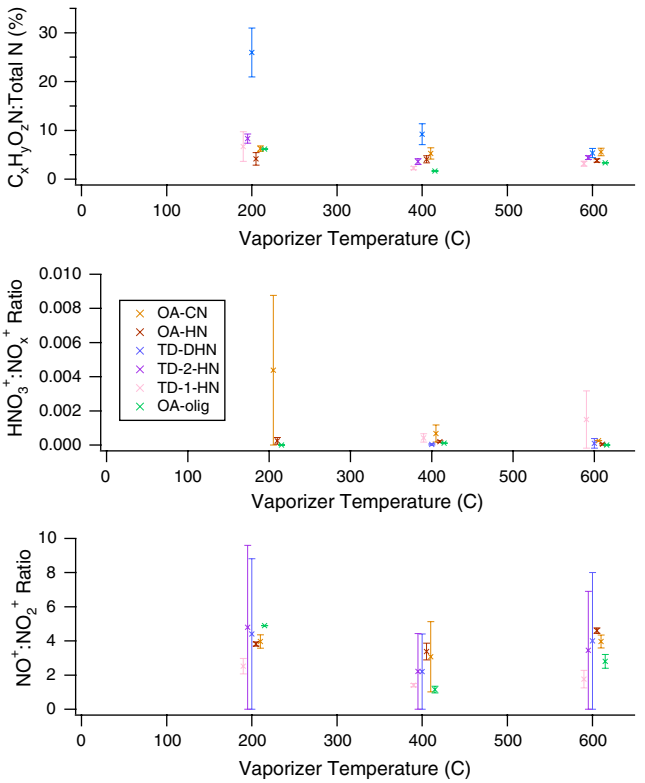


**Fig. S6.** The relative contribution of organonitrogen fragments to total N detected, $HNO_3^+/NO_x^+$ ratio, and $NO^+/NO_2^+$ ratio as a function of vaporizer temperature ($T_v$) in each of five standards, including the mix of oleic acid-derived oligomers, carbonyl nitrates, and hydroxy nitrates (uncertainty is standard error the mean). Vaporizer temperatures were 200, 400, and 600 °C for all standards, but are presented offset by ±5–15° for comparison purposes.

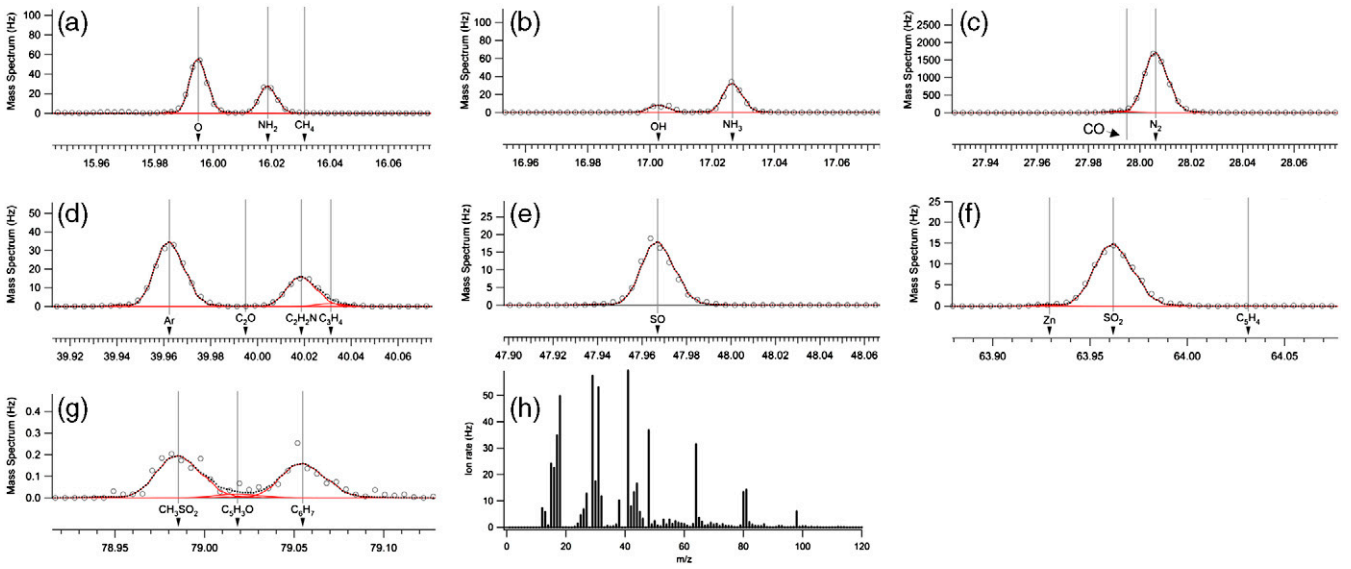


**Fig. S7.** High-resolution mass spectra (*a*–*g*) at select S-containing *m*/*z* ratios, along with *m*/*z* 28 and 40, for the organosulfate (OS) standard taken taken at $T_v = 600\,°C$. The complete mass spectrum (*h*) is presented at unit mass resolution.

**Table S1. Fragmentation pattern of $NH_4NO_3$ and ON standards in the HR-AMS at $T_v = 600\,°C$ and fragmentation of $(NH_4)_2SO_4$ (1) and organic sulfate (this study) standards in the HR-AMS at $T_v = 600\,°C$, presented as relative signal intensity**

| | $NH_4NO_3$ | ON standards | | | | | |
|---|---|---|---|---|---|---|---|
| | | OlA-HN | OlA-CN | OlA-olig | TD-DHN | TD-2OH HN | TD-1OH HN |
| $NO^+$ | 100 | 100 | 100 | 100 | 100 | 100 | 100 |
| $NO_2^+$ | 65 | 22 | 25 | 36 | 25 | 29 | 57 |
| $HNO_3^+$ | 0.4 | 0.04 | 0.4 | 0.3 | — | — | — |
| O/C raw | | 0.15 | 0.18 | 0.18 | 0.18 | 0.22 | 0.22 |
| O/C calibrated | | 0.2 | 0.24 | 0.24 | 0.24 | 0.29 | 0.29 |
| O/C cal. w/o $NO_x^+$ | | 0.11 | 0.11 | 0.09 | 0.11 | 0.11 | 0.08 |
| O/C molecular | | 0.33 | 0.33 | — | 0.36 | 0.29 | 0.29 |
| H/C raw | | 1.66 | 1.66 | 1.69 | 1.72 | 1.76 | 1.75 |
| H/C calibrated | | 1.82 | 1.82 | 1.86 | 1.89 | 1.93 | 1.92 |
| H/C molecular | | 1.94 | 1.83 | — | 2.07 | 2.07 | 2.07 |
| N/C raw | | 0.03 | 0.04 | 0.04 | 0.04 | 0.05 | 0.04 |
| N/C calibrated | | 0.03 | 0.04 | 0.04 | 0.04 | 0.05 | 0.04 |
| N/C cal. w/o $NO_x^+$ | | 0.0009 | 0.0009 | 0.0007 | 0.0009 | 0.0007 | 0.0004 |
| N/C molecular | | 0.06 | 0.06 | — | 0.07 | 0.07 | 0.07 |

| | | OS standards | |
|---|---|---|---|
| Fragment | Mass | $(NH_4)_2SO_4$ | $C_5H_{11}O_7S$ (OS) |
| S | 31.9721 | 14 | 19 |
| SO | 47.9670 | 67 | 100 |
| $SO_2$ | 63.9619 | 100 | 75 |
| $HSO_2$ | 64.9697 | 6 | 8 |
| $CH_3SO_2$ | 78.9854 | — | 1 |
| $SO_3$ | 79.9568 | 57 | 37 |
| $HSO_3$ | 80.9646 | 26 | 34 |
| $H_2SO_4$ | 97.9674 | 17 | 14 |

Atomic ratios (the number of oxygen, hydrogen, or nitrogen atoms relative to carbon atoms: O/C, H/C, N/C) determined by elemental analysis of HR-AMS data, including $H_xN_yO_z^+$, are shown for each ON standard as raw (experimental, no corrections applied), calibrated (corrected by Aiken et al. (2008) typically used for AMS elemental analyses) and molecular atomic ratios. Atomic ratios determined without $NO_x^+$ fragments (cal. w/o $NO_x^+$) are also presented for each standard. $(NH_4)_2SO_4$ standards were taken at unit mass resolution, and include the $^{33}SO_2$ isotope and $^{33}SO_3$ isotope for $HSO_2$ and $HSO_3$, respectively (1).

OlA-HN: $CH_3(CH_2)_7CH(OH)CH(ONO_2)(CH_2)_7C(O)OH + CH_3(CH_2)_7CH(ONO_2)CH(OH)(CH_2)_7C(O)OH$

OlA-CN: $CH_3(CH_2)_7C(O)CH(ONO_2)(CH_2)_7C(O)OH + CH_3(CH_2)_7CH(ONO_2)C(O)(CH_2)_7C(O)OH$

TD-DHN: $CH_3(CH_2)_8CH(ONO_2)(CH_2)_2CH(OH)CH_2OH + CH_3(CH_2)_9CH(ONO_2)CH_2CH(OH)CH_2OH$

TD-2OH HN: $CH_3(CH_2)_{11}CH(OH)CH_2ONO_2$

TD-1OH HN: $CH_3(CH_2)_{11}CH(ONO_2)CH_2OH$